Available online at www.sciencedirect.com
SCIENCE DIRECT
Fusion Engineering and Design 81 (2006) 909–916
Fusion Engineering and Design
www.elsevier.com/locate/fusengdes

Ferritic steel-blanket systems integration R&D—Compatibility assessment

A. Kimura [a,*], R. Kasada [a], A. Kohyama [a], S. Konishi [a], M. Enoeda [b], M. Akiba [b], S. Jitsukawa [c], S. Ukai [d], T. Terai [e], A. Sagara [f]

[a] *Institute of Advanced Energy, Kyoto University, Gokasho, Uji, Kyoto 611-0011, Japan*
[b] *Naka Fusion Research Establishment, Japan Atomic Energy Research Institute, 801-1 Mukoyama, Naka-machi, Naka-gun, Ibaraki-ken 311-0193, Japan*
[c] *Tokai Research Establishment, Japan Atomic Energy Research Institute, 2-4 Shirane, Tokai-mura, Naka-gun, Ibaraki-ken 319-1195, Japan*
[d] *O-arai Engineering Center, Japan Nuclear Cycle Institute, 4002 Narita-cho O-arai-machi, Higashi-ibaraki-gun, Ibaraki-ken 311-1393, Japan*
[e] *Graduate School of Engineering, The University of Tokyo, Hongo, Bunkyo-ku, Tokyo 113-8656, Japan*
[f] *National Institute of Fusion Science, National Institute of Natural Science, Oroshi-cho, Toki, Gifu 509-5292, Japan*

Received 10 May 2005; received in revised form 5 September 2005; accepted 5 September 2005
Available online 10 January 2006

Abstract

The reduced activation ferritic steel (RAFS) has been selected as structural material for a variety of blanket systems for ITER test blanket modules (TBM). In the evaluation of integrated performance of ferritic steels as structural components of blanket systems, there are unique issues as well as common issues for each blanket system. One of the unique issues for each system is the compatibility of ferritic steels with the coolant materials. The corrosion rate of ferritic steels in hot water, super critical pressurized water (SCPW), humid air, Pb–17Li, lithium and Flibe at various temperatures is reviewed in this work. Efforts to improve corrosion resistance have been made, taking the alloy design into account. A dispersion of yttria was effective to improve corrosion resistance of a RAFS. The compatibilities of RAFSs with hot water, Pb–17Li, lithium and Flibe are considered to be good enough for the TBM applications. The liquid metal embrittlement (LME) is considered to be a critical issue for the utilization of RAFSs for the lithium systems. Several issues towards DEMO and beyond are shown from the compatibility point of view.

Keywords: Ferritic steels; Test blanket modules; Compatibility; Water; Liquid metals; Salt

1. Introduction

In the test blanket working group (TBWG) as an activity of the International Energy Association (IEA),

* Corresponding author. Tel.: +81 774 38 3476; fax: +81 774 38 3479.
E-mail address: kimura@iae.kyoto-u.ac.jp (A. Kimura).

0920-3796/$ – see front matter © 2005 Elsevier B.V. All rights reserved.
doi:10.1016/j.fusengdes.2005.09.018

a variety of ITER test blanket modules (TBMs) have been proposed by each party: helium-cooled ceramic (WSG-1), helium-cooled LiPb (WSG-2), water-cooled ceramic (WSG-3), self-cooled lithium (WSG-4) and self-cooled molten salt (WSG-5) blanket systems [1]. Among the three candidate fusion structural materials, the reduced activation ferritic steel (RAFS) has been selected as structural material for almost all the above blanket systems for ITER–TBM [2]. This is because the maturity of the RAFS as a structural material is currently way beyond the others, especially from the point of manufacturing techniques, industrial productivity, materials database, total-performance, and so on. The chemical compositions of the RAFSs are shown in Table 1 with some other ferritic–martensitic steels.

However, the targeted structural materials for DEMO and beyond have been considered to be the silicon carbide composite (SiC/SiC) [3] for WSG-1 and 2, the RAFS and the oxide dispersion strengthening steel (ODSS) [4] for WSG-3, the vanadium alloy [5] for WSG-4, and the RAFS and ODSS [6] for WSG-5. Thus, some materials-blanket system integration issues have not been fully discussed yet for the blanket systems made of the RAFS. One of the critical issues is the compatibility of the RAFS with a variety of coolant materials.

In this work, the compatibility of the RAFS with each coolant material is reviewed and assessed for the applications to ITER–TBM and beyond.

2. Solid breeder systems

2.1. Pressurized water

As a measure of the corrosion resistance, the passive current density in high-pressure water at 523 K was measured for iron–chromium alloys and some steels to investigate the corrosion resistance of ferritic–martensitic steels [7]. The results are summarized in Fig. 1, indicating that the corrosion resistance remarkably depends on the chromium concentration in the materials [8]. In comparison with an austenitic stainless steel (SUS304), the ferritic steels containing 9–10% Cr showed the five times larger current density, namely higher corrosion rate, which may apply to the RAFS that contains 9% Cr. It is well known that the increase in the Cr concentration improves corrosion resistance, but decreases fracture toughness with and without irradiation. However, the previous irradiation experiments clearly showed that the irradiation embrittlement became a minimum at the chromium concentrations ranging from 7 to 9% [8–11]. Furthermore, the steels containing 7–9% Cr have a martensitic single phase structure that is favorable to keep

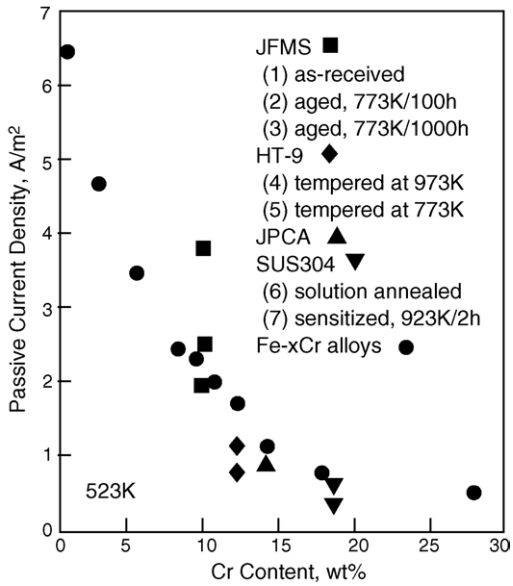

Fig. 1. The dependence of the corrosion rate in pressurized water at 523 K on the Cr content of the steels and Fe–*x*Cr alloys.

Table 1
The chemical compositions of the ferritic–martensitic steels

wt.%	C	Si	Mn	Cr	W	V	Ta	Mo	Ni	Nb
F82H	0.09	0.13	0.16	7.7	1.95	0.16	0.04	–	0.04	–
JLF-1	0.1	<0.1	0.46	9.04	1.97	0.2	0.07	<0.01	–	–
EUROFER 97	0.1	0.05	0.44	8.8	1.15	0.2	0.07	0.003	–	0.002
Optifer Ia	0.11	0.06	0.57	8.5	1.16	0.23	0.07	0.005	0.005	0.009
1.4914	0.13	0.37	0.82	10.6	–	0.22	–	0.77	0.87	0.16
FTT-9	0.2	0.22	0.5	11.8	0.5	0.29	–	0.99	0.48	–

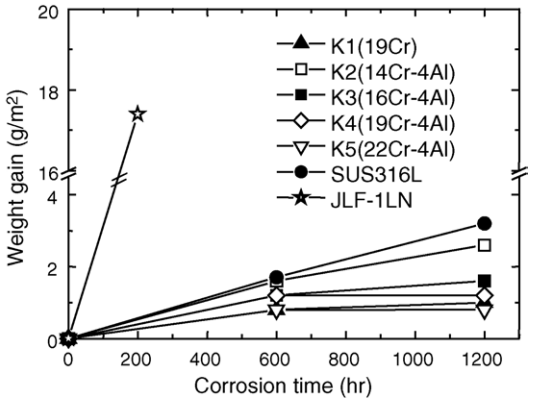

Fig. 2. The weight gains of the high-Cr ODS ferritic steels as well as those of a 9Cr martensitic steel (JLF-1LN) and an austenitic stainless steel (SUS316L) in super critical pressurized water (783 K, 25 MPa). The ODS steels show a better corrosion resistance than SUS316L.

high-creep strength at elevated temperatures. Increasing the Cr concentration to more than 9% leads to the formation of δ-ferrite phase in the martensite phase, reducing the creep strength. Since the fracture toughness was considered to be more critical than the corrosion resistance in fusion blankets, the 9% Cr RAFS was selected as the prime candidate blanket structural material [8–20].

The uniform corrosion test results showed that the weight loss of a RAFS, F82H, was 6 g/m^2 at 533 K for 2600 h [21]. The F82H never showed the stress corrosion cracking (SCC) in as-received and normalized-and-tempered conditions, but the hardened martensite with a hardness HV > 340 or ultimate tensile strength >1100 MPa suffered from IGSCC [21]. According to the recent results on SCC tests for the ODSS, however, no SCC was observed for the ODSS (Fig. 2) with an ultimate strength >900 MPa, as shown in Fig. 3 [22].

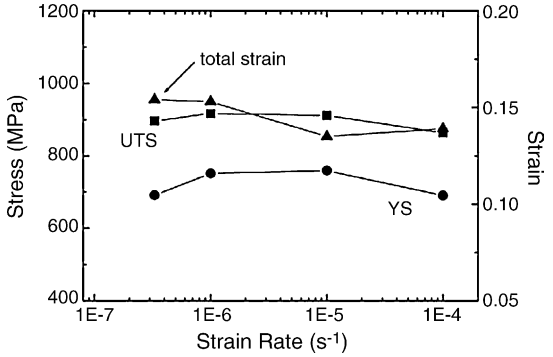

Fig. 3. The dependence of the total strain, ultimate tensile strain (UTS) and yield stress (YS) of the 19Cr–4Al-ODS steel on the strain rate tested in the hot pressurized water (288 °C, 7.8 MPa). No dependence of the properties on the strain rate indicates low susceptibility to SCC.

2.2. Super-critical pressurized water

High-temperature operation is demanded for a high thermal efficiency of the plants. Since the RAFS limits the operation temperature to 823 K, the advanced ferritic steels such as the ODSS have been developed [23–25]. The corrosion rate in super-critical pressurized water (SCPW) (783 K, 25 MPa) was measured for several kinds of the steels by means of weight loss (and gain) measurements. Nine ODS steels were investigated: a 12Cr-ODS steel, three 9Cr-ODS steels and five high-chromium ODS steels of which the titanium and yttrium concentrations were partly altered [26]. The chemical compositions of the ODS steels are shown in Table 2.

Fig. 2 shows the dependence of weight gain on the corrosion test period in each the steel. The weight gain of the RAFS, JLF-1, attained 800 g/m^2 for 200 h. The 9% Cr-ODS steel of the first generation of ODS steels

Table 2
The chemical compositions of ODS steels (wt.%)

Materials	C	Si	Mn	Cr	W	Al	Ti	N	Y	Y_2O_3
12Cr-ODS	0.02	0.05	0.046	11.97	2.02	–	0.30	0.010	0.19	0.24
9Cr-ODS(1)	0.13	0.05	0.044	9.00	1.95		0.20	0.013	0.29	0.37
9Cr-ODS(2)	0.13	0.006	0.01	9.11	1.95	–	0.18	0.017	–	–
9Cr-ODS(3)	0.13	0.005	0.01	8.84	1.91		0.29	0.010	0.35	0.44
19Cr(K1)	0.05	0.041	0.06	18.37	0.29	<0.01	0.28	0.014	0.29	0.368
13Cr–4Al(K2)	0.04	0.033	0.06	13.64	1.65	4.12	0.28	0.009	0.30	0.381
19Cr–4Al(K3)	0.08	0.033	0.06	16.00	1.82	4.59	0.28	0.006	0.29	0.368
16Cr–4Al(K4)	0.09	0.039	0.06	18.85	1.83	4.61	0.28	0.005	0.29	0.368
22Cr–4Al(K5)	0.10	0.039	0.07	22.05	1.80	4.55	0.27	0.005	0.28	0.356

is almost the same as that of a ferritic/martensitic steel. In comparison with the first generation of the ODS steels, the second generation of high-Cr ODS steels (>14% Cr) showed a high corrosion resistance better than an austenitic stainless steel (SUS316) [27,28]. Furthermore, an increase of chromium and an addition of aluminum at the same time resulted in further suppression of corrosion. It shows that the additions of chromium over 14 wt.% and aluminum (4.5 wt.%) are very effective in suppressing corrosion in SCPW. This is considered to be due to the formation of Al_2O_3 or the suppression of the formation of Fe_2O_3 [29,30]. As for the SCC in SCPW, the recent research revealed that the susceptibility to SCC is smaller in SCPW (783 K, 25 MPa) than in a pressurized water (563 K, 7.8 MPa).

2.3. Humid air

For the application to gas-cooled systems, high-temperature strength and oxidation are considered to be critical for the RAFS. In the DEMO reactors, the ODSS could be applicable for the systems because of its high-temperature strength. As for the oxidation resistance, the loss of mass by oxidation in humid air at 1023 K of the ODSS was considerably smaller than that of the 11% Cr-ferritic steels, and almost similar to that of the austenitic stainless steel (SUS316), as shown in Fig. 4, although the concentration of Cr in the ODSS was only 9%. This suggests that the oxidation was suppressed by the dispersion of nano-scaled yttria particles [31]. Furthermore, the yttria particles may play a role to increase the tritium trapping capacity. It is expected that a dense dispersion of nano-sized yttria particles in the surface region will work as a kind of barrier to reduce corrosion and tritium permeation.

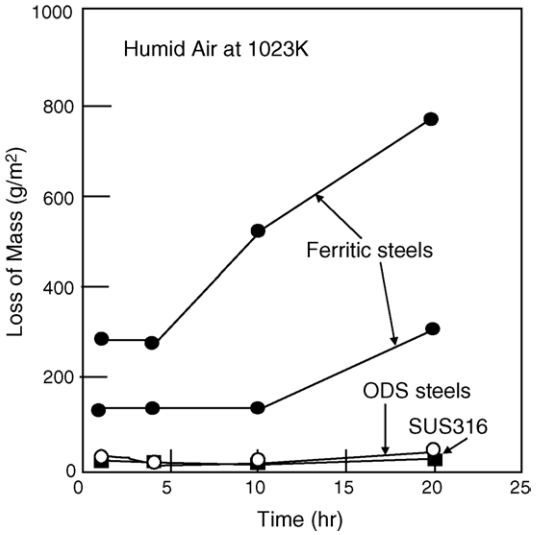

Fig. 4. The loss of mass by oxidation in humid air at 1023 K of the 9%Cr-ODSS (○) was considerably smaller than that of the 11%Cr-ferritic steels (●), and almost similar to that of the austenitic stainless steel (SUS316) (■).

3. Liquid breeder systems

3.1. Liquid metals

The difference in the chemical potentials of the alloying elements in between liquid metal and material may cause the solution of the elements into liquid metals. The solubility values of the major steel elements are shown in Table 3 [32–34]. The solubility value of nickel in lead is very high, suggesting that austenitic stainless steels and nickel base alloys are inadequate for Pb–17Li systems.

3.1.1. Pb–17Li

Several corrosion tests were carried out on ferritic and austenitic steels in liquid Pb–17Li. It was confirmed that the corrosion rate of the ferritic–martensitic steels was five times slower than that of the SUS316 steel [36]. The past data is summarized in Table 4 [35–40] with those tested in lithium [37,41]. Although the test periods were limited to 6000 h at most in the temperature range from 723 to 823 K, the evaluated corrosion rate of ferritic–martensitic steels is less than 100 μm/year below 755 K. It should be noticed that the corrosion rate significantly increases with increasing the test temperature: 370 μm/year at 873 K [35]. As for the flow rate effect, high flow rates resulted in a high corrosion rate, indicating that the flow rate could be small to reduce the corrosion rate as well as the influence of the magnetohydrodynamic (MHD) pressure drop.

The stress corrosion cracking in liquid metals or liquid metal embrittlement (LME) is another critical issue. Sample et al. investigated the tensile deformation and fracture behavior of ferritic–martensitic steels in Lb–17Li at temperatures from 523 to 723 K [42–46].

Table 3
The solubility values of the major steel elements in liquid metals

Temperature (K)	LM	Fe (wt. ppm)	Cr (wt. ppm)	Ni (wt. ppm)
673	Li	1	1	45
	Na	0.05	0.0001	0.5
	Pb	0.2–0.8	0.002	1800
773	Li	4	4	200
	Na	0.4	0.005	0.9
	Pb	0.8–2.5	0.1	3500
973	Li	12	13	22
	Na	42	43	40
	Pb	370	2%	11%
873	Pb–17Li	3.7		5.60%

Table 4
Summary of the corrosion data of the ferritic–martensitic steels in Pb–17Li and lithium

LM	Materials	Temp. (K)	Flow rate	Exposure time (h)	Loss of metal	Estimated corrosion depth (mm/year)	Ref.
Pb–17Li	1.4914	823	0.3 m/s	3700	200 mm	370	[35]
Pb–17Li	1.4914, HT9	723	0.1 m/s	3000	7 mm	30	[36]
Pb–17Li	Fe-12(9)Cr-6.5 Mn(0.5 V)-1(0)W	755	0.35 L/min	2000	40 g/m^2	20	[37]
Pb–17Li	Optifer, MANET1, F82H-mod.	753	0.3 m/s	6000	80 mm	100	[38]
Pb–17Li	EUROFER 97	723	0.01 m/s	4500	–	40	[39]
Pb–17Li	EUROFER 97	773	25 mm/s	2500	10 g/m^2	–	[40]
Li	Fe-12(9)Cr-6.5(2.5)Mn-1 W	755	1 L/min	4000	4 g/m^2	0.5	[37]
Li	12Cr-1Mo	873	25 mm/s	7000	20 g/m^2	2.5	[41]

Table 5
Summary of tensile test results of the ferritic–martensitic steels in Pb–17Li

LM	Materials	Temp. (K)	Deformation rate (/s)	Loss of ductility	Ref.
Pb–17Li	1.4914	523, 573	$>8 \times 10^{-4}$	No	[42]
Pb–17Li	1.4914, HT9	523	2.8×10^{-7}	No	[43]
Pb–17Li	Optifer, MANET1, F82H-mod.	523, 673	1.1×10^{-4}	Weld	[44]
Pb–17Li	EUROFER 97	523, 673	1.1×10^{-4}	Weld	[45]
Pb–17Li	EUROFER 97	723	3×10^{-3}	No	[39]

The test results are summarized in Table 5. The results showed that almost no indication of LME was shown in the tensile behavior of the ferritic–martensitic steels, although a serrated flow was observed in a slow strain rate test at 2.8×10^{-7}/s [43]. However, the weld metals without post-weld heat treatment (PWHT) suffered from LME showing the reduction of total elongation [44,45]. It was reported that the PWHT at an adequate temperature was inevitable to avoid the LME, and that the investigation is necessary to assess the potential of the LME for the irradiation-hardened ferritic–martensitic steels. It is also considered that a synergism of liquid metal, irradiation and hydrogen/helium may appear in the fracture behavior of the stressed metallic materials.

3.1.2. Lithium

As expected from Table 3, the mass transfer between the RAFS and liquid lithium would not be so marked as that for Pb–17Li. Actually, the corrosion test results, which are limited, indicate that the corrosion rate of the ferritic–martensitic steels in lithium is more than one order of magnitude lower than in Pb–17Li. Again, the corrosion resistance is better than the SUS316 steel [41]. It was also reported that the 9Cr-steel showed better resistance than the 12Cr-steel [37]. In lithium, a sufficiently high nitrogen activity results in the formation of Li_9CrN_5 that enhances the intergranular corrosion. Oxygen is not expected to influence the corrosion behavior because of the stability of Li_2O. However, the oxide film covering a steel surface is easily removed in a lithium environment.

Although it is well known that many metals suffer from LME in liquid lithium, no data was available for the RAFS. In general, the LME occurs under the application of stress higher than the yield stress, and the fracture mode is intergranular. Surface oxide films often suppress the LME. The mechanisms proposed for the LME are: (1) stress-assisted solution; (2) formation of intermetallics at the crack tip; (3) atomic-bond decohesion; (4) reduction of surface energy.

3.2. Flibe

The corrosion experiment of the RAFSs in Flibe is very limited [46–48]. Terai and co-workers [46–48] conducted a dipping experiment at 823 K to observe the corrosion behavior of ferritic steels such as SUS430 (18 wt.% Cr) and JLF-1 (9 wt.% Cr) in Flibe under Ar gas environment, and reported that the oxide layer formed in 72 h on SUS430 mainly consisted of Cr_2O_3, which was considered to prevent a severe oxidation. As for JLF-1, a RAFS, similar dipping experiments but under the Ar gas environments with 1% oxygen (720 h) or with 82 ppm HF (216 h) were carried out. It was reported that the oxidation behavior was influenced by the oxygen concentration, but not by the existence of the HF. In the case of very low oxygen concentration, a dense Cr_2O_3 film was formed, while in the case of Ar + 1% O_2, a spinel type oxide $(Fe, Cr)_3O_4$ was formed. Finally, they concluded that the compatibility of JLF-1 with Flibe was good for the first 720 h. No data is available for the SCC of ferritic steels in molten salts.

4. Summary

The compatibilities of the RAFSs with the candidate coolant materials, such as pressurized water, SCPW, humid air, Pb–17Li, lithium and Flibe, were reviewed and assessed for the application to ITER–TBM and beyond. It is said that the RAFS can be employed as structural material of a variety of cooling systems of ITER–TBM without any coating. However, some issues should be solved for DEMO and beyond.

1) Water and humid air: The compatibility was influenced by the Cr concentration in the steels. The nano-scaled yttria particles are effective to reduce the corrosion and the tritium permeation. Surface modification of the RAFS, such as Cr concentration gradient together with dispersing nano-sized yttria particles, is considered to be effective to solve the corrosion and tritium permeation issues. SCC will not be crucial for the RAFS, but the surface modification may enhance it.
2) Pb–17Li: High-temperature operation >873 K will be limited by corrosion. A ceramic coating or ceramic insert will be necessary. Application of silicon carbide composite (SiC/SiC) as insert plates will be effective to solve this issue. The LME will be one of the issues.
3) Lithium: The compatibility will be good enough. The susceptibility to LME will be very high. The MHD pressure drop should be solved by ceramic

coating or inserting, which also solve the issue of the LME.

4) Flibe: The compatibility seems to be good for 720 h at 823 K. However, long-term corrosion experiments are necessary. The control of TF concentration will be one of the critical issues.

References

[1] Minutes of 12th Test Blanket Working Group (TBWG-12), ITER-JWS, Garching, July 2003.

[2] Minutes of 13th Test Blanket Working Group (TBWG-13), ITER-JWS, Garching, July 2004.

[3] L.V. Boccaccini, L. Giancarli, G. Janeschitz, S. Hermsmeyer, Y. Poitevin, A. Cardella, E. Diegele, Materials and design of the European DEMO blankets, J. Nucl. Mater. 329–333 (2004) 148–155.

[4] A. Kimura, Reduced activation ferritic steel R&D based on Jupiter-1 results, Fusion Sci. Tech. 44 (2) (2003) 480–484.

[5] R.J. Kurtz, K. Abe, V.M. Chernov, D.T. Hoelzer, H. Matsui, T. Muroga, G.R. Odette, Recent progress on development of vanadium alloys for fusion, J. Nucl. Mater. 329–333 (2004) 47–55.

[6] A. Sagara, O. Motojima, K. Watanabe, S. Imagawa, H. Yamanishi, O. Mitarai, T. Satow, H. Tikaraishi, FFHR Group, Blanket and divertor design for force free helical reactor (FFHR), Fus. Eng. Des. 29 (1995) 51–56.

[7] T. Misawa, Y. Hamaguchi, M. Saito, Stress corrosion cracking and hydrogen embrittlement studies of austenitic and ferritic steels by small punch test, J. Nucl. Mater. 155–157 (1988) 749–753.

[8] A. Kimura, H. Kayano, T. Misawa, H. Matsui, Designation of alloy composition of low activation martensitic steels, J. Nucl. Mater. 212–215 (1994) 690–694.

[9] A. Kohyama, A. Hishinuma, D.S. Gelles, R.L. Klueh, W. Dietz, K. Ehrlich, Low-activation ferritic and martensitic steels for fusion application, J. Nucl. Mater. 233–237 (1996) 138–147.

[10] R.L. Klueh, D.S. Gelles, S. Jitsukawa, A. Kimura, G.R. Odette, B. van der Schaaf, M. Victoria, Ferritic/martensitic steels—overview of recent results, J. Nucl. Mater. 307–311 (2002) 455–465.

[11] B. van der Schaaf, D.S. Gelles, S. Jitsukawa, A. Kimura, R.L. Klueh, A. Moslang, G.R. Odette, Progress and critical issues of reduced activation ferritic/martensitic steel development, J. Nucl. Mater. 283–287 (2000) 52–59.

[12] A. Hishinuma, A. Kohyama, R.L. Klueh, D.S. Gelles, W. Dietz, K. Ehrlich, Current status and future R&D for reduced-activation ferritic/martensitic steels, J. Nucl. Mater. 258–263 (1998) 193–204.

[13] A. Kimura, A. Kohyama, K. Shiba, R.L. Klueh, D.S. Gelles, G.R. Odette, Reduced activation ferritic steel R&D in US/Japan collaborative research, 2001 Fusion Energy 2000, in: Proc. 18th Int. Conf. Sorrento, 2000, IAEA, Vienna, CD-ROM file and http://www.iaea.org/programmes/ripc/physics/fec2000/html/node1.htm.

[14] A. Kimura, M. Narui, T. Misawa, H. Matsui, A. Kohyama, Dependence of impact properties on irradiation temperature in reduced-activation martensitic steels, J. Nucl. Mater. 258–263 (1998) 1340–1344.

[15] S. Jitsukawa, A. Kimura, A. Kohyama, R.L. Klueh, A.A. Tavassoli, B. van der Schaaf, G.R. Odette, J.W. Rensman, M. Victoria, C. Petersen, Recent results of the reduced activation ferritic/martensitic steel development, J. Nucl. Mater. 329–333 (2004) 39–46.

[16] A. Kimura, H. Kayano, S. Ohta, Irradiation induced suppression of creep in a low activation 9%Cr–2%W steel, J. Nucl. Mater. 179–181 (1991) 741–744.

[17] H. Kayano, A. Kimura, M. Narui, T. Kikuchi, S. Ohta, Effects of small changes in alloy composition on the mechanical properties of low activation 9%Cr–2%W steel, J. Nucl. Mater. 179–181 (1991) 671–674.

[18] A. Kimura, R. Kasada, R. Sugano, A. Hasegawa, H. Matsui, Annealing behavior of irradiation hardening and microstructure in helium-implanted reduced activation martensitic steel, J. Nucl. Mater. 283–287 (2000) 827–831.

[19] A. Kimura, R. Kasada, K. Morishita, R. Sugano, A. Hasegawa, K. Abe, T. Yamamoto, H. Matsui, N. Yoshida, B.D. Wirth, T.D. Rubia, High resistance to helium embrittlement in reduced activation martensitic steels, J. Nucl. Mater. 303–307 (2002) 521–526.

[20] A. Kohyama, Y. Kohno, M. Kuroda, A. Kimura, F. Wan, Production of low activation steel; JLF-1, large heats–current status and future plan, J. Nucl. Mater. 258–263 (1998) 1319–1323.

[21] J. Lapena, F. Blazqez, Water corrosion of F82H-modified in simulated irradiation conditions by heat treatment, J. Nucl. Mater. 283–287 (2000) 1341–1345.

[22] H.S. Cho, H. Ohkubo, N.Y. Iwata, A. Kimura, S. Ukai, M. Fujiwara, Evaluation of susceptibility to stress corrosion cracking of oxide dispersion strengthening steels in hot pressurized water, in: Proc. Int. Cong. on Advances in Nuclear Power Plants, ICAPP-2005, CD-ROM file, paper 5457.

[23] S. Ukai, T. Nishida, T. Okuda, T. Yoshitake, Development of oxide dispersion strengthened ferritic martensitic steels, J. Nucl. Sci. Technol. 35 (1998) 294–300.

[24] S. Ukai, T. Nishida, T. Okuda, T. Yoshitake, R&D of oxide dispersion strengthened ferritic martensitic steels for FBR, J. Nucl. Mater. 258–263 (1998) 1745–1749.

[25] A. Kimura, S. Ukai, M. Fujiwara, Oxide dispersion strengthening steels R&D for advanced water-cooling nuclear systems, in: Proc. Int. Cong. on Advances in Nuclear Power Plants, ICAPP-2004, ISBN: 0-89448-680-2, CD-ROM file, paper 2070.

[26] H.S. Cho, A. Kimura, S. Ukai, M. Fujiwada, Corrosion properties of oxide dispersion strengthened steels in supercritical water environment, J. Nucl. Mater. 329–333 (2004) 387–391.

[27] A. Kimura, S. Ukai, M. Fujiwara, Development of fuel clad materials for high burn-up operation of LWR, in: Proc. Int. Conf. on Global Environment and Advanced Nuclear Power Plants, GENES4/ANP2003, ISBN: 4-901332-01-5, CD-ROM file, paper 1198.

[28] J.S. Lee, A. Kimura, S. Ukai, M. Fujiwara, Effects of hydrogen on the mechanical properties of oxide dispersion strengthening steels, J. Nucl. Mater. 329–333 (2004) 1122–1126.
[29] B.A. Pint, I.G. Wright, Long-term high temperature oxidation behavior of ODS ferritics, J. Nucl. Mater. 307–311 (2002) 763–768.
[30] P.Y. Hou, J. Stringer, The effect of reactive element additions on the selective oxidation, growth and adhesion of chromia scales, Mater. Sci. Eng. A 202 (1995) 1–10.
[31] T. Kaito, T. Narita, S. Ukai, Y. Matsuda, High temperature oxidation behavior of ODS steels, J. Nucl. Mater. 329–333 (2004) 1388–1392.
[32] M.W. Leabenworth, R.E. Cleary, The solubility of Ni, Cr, Fe, Ti and Mo in liquid lithium, Acta Metall. 9 (1961) 519–520.
[33] R.M. Singers, Corrosion by Liquid Metals, Plenum Press, New York, 1970, 561.
[34] H.U. Bolgstedt, H. Feuerstein, The solubility of metals in Pb–17Li liquid alloy, J. Nucl. Mater. 191–194 (1992) 988–991.
[35] H.U. Borgstedt, G. Drechsler, G. Frees, Z. Peric, Corrosion testing of steel X 18 CrMoVNb 12 1 (1.4914) in A Pb–17Li pumped loop, J. Nucl. Mater. 155–157 (1988) 728–731.
[36] M. Broc, T. Flament, P. Fauvet, J. Sannier, Corrosion of austenitic and martensitic stainless steels in flowing 17Li–83Pb alloy, J. Nucl. Mater. 155–157 (1988) 710–714.
[37] O.K. Chopra, D.L. Smith, Compatibility of ferritic steels in forced circulation lithium and Pb–17Li systems, J. Nucl. Mater. 155–157 (1988) 715–721.
[38] H. Glasbrenner, J. Konys, H.D. Röhrig, K. Stein-Fechner, Z. Voss, Corrosion of ferritic–martensitic steels in the eutectic Pb–17Li, J. Nucl. Mater. 283–287 (2000) 1332–1335.
[39] G. Benamati, C. Fazio, I. Ricapito, Mechanical and corrosion behaviour of EUROFER 97 steel exposed to Pb–17Li, J. Nucl. Mater. 307–311 (2002) 1391–1395.
[40] K. Splichal, M. Zmitko, Corrosion behaviour of EUROFER in Pb–17Li at 500 °C, J. Nucl. Mater. 329–333 (2004) 1384–1387.
[41] F. Tortorelli, Corrosion of ferritic steels by molten lithium: influence of competing thermal gradient mass transfer and surface product reactions, J. Nucl. Mater. 155–157 (1988) 722–727.
[42] V. Coen, H. Kolbe, L. Orecchia, Effects of Pb–17Li on the tensile properties of steels, J. Nucl. Mater. 155–157 (1988) 740–743.
[43] T. Sample, V. Coen, H. Kolbe, L. Orecchia, The effects of hydrogen and Pb–17Li on the tensile properties of 1.4914 martensitic steel, J. Nucl. Mater. 191–194 (1992) 960–964.
[44] T. Sample, P. Fenici, H. Kolbe, Liquid metal embrittlement susceptibility of welded MANET II (DIN 1.4914) in liquid Pb–17Li, J. Nucl. Mater. 233–237 (1996) 244–247.
[45] T. Sample, H. Kolbe, Liquid metal embrittlement (LME) susceptibility of the 8–9% Cr martensitic steels F82H-mod., OPTIFER IVb and their simulated welded structures in liquid Pb–17Li, J. Nucl. Mater. 283–287 (2000) 1336–1340.
[46] T. Terai, Y. Hosoya, S. Tanaka, A. Sagara, O. Motojima, Compatibility of structural materials with Li_2BeF_4 molten salt breeder, J. Nucl. Mater. 258–263 (1998) 513–518.
[47] H. Nishimura, T. Terai, T. Yoneoka, S. Tanaka, A. Sagara, O. Motojima, Compatibility of structural candidate materials with LiF–BeF_2 molten salt mixture, J. Nucl. Mater. 283–287 (2000) 1326–1331.
[48] H. Nishimura, T. Terai, M. Yamawaki, S. Tanaka, A. Sagara, O. Motojima, Compatibility of ferritic steels with Li_2BeF_4 molten salt breeder, J. Nucl. Mater. 307–311 (2002) 1355–1359.